# Contributions of Polygenic Risk for Obesity to PTSD-Related Metabolic Syndrome and Cortical Thickness

## Supplementary Materials

### Genotyping

Laboratory Procedures.

Whole blood peripheral samples were obtained and DNA extracted from buffy coat. DNA was isolated on a Qiagen AutoPure instrument with Qiagen reagents; concentrations were normalized using the Quant-iT™ PicoGreen dsDNA fluorescent assay (Invitrogen). DNA quality and quantity were ascertained by the TaqMan® RNase P Detection assay (Applied Biosystems Assay, Life Technologies, Carlsbad, CA) with fluorescence detection on a 7900 Fast Real Time PCR System (Applied Biosystems, Life Technologies, Carlsbad, CA) according to the manufacturer's protocol. DNA samples were whole-genome amplified, fragmented, precipitated and resuspended prior to hybridization on Illumina HumanOmni2.5-8 beadchips for 20 hours at $48^0$C according to the manufacturer's protocol (Illumina, San Diego, CA). After hybridization, a single-base extension followed by a multi-layered staining process was conducted. Beadchips were imaged using the Illumina iScan System and analyzed with Illumina GenomeStudio v2011.1 software containing Genotyping v1.9.4 module. A GenomeStudio project was created with a custom genotyping cluster file, and call rates were >0.994 for all samples. Technical replicates had genotyping reproducibility error rates <0.0005 prior to SNP data cleaning.

Obesity Polygenic Risk Score (PRS).

GWAS results from Speliotes et al. (2010) were downloaded from the following website: http://portals.broadinstitute.org/collaboration/giant/index.php/Main_Page. Imputation of ungenotyped SNPs was performed using IMPUTE2 (Howie et al., 2012) and the EUR 1000 genomes phase 1 reference data (The 1000 Genomes Project Consortium, 2012).

### MRI Processing

FreeSurfer Cortical Thickness Pipeline

The technical details of these procedures are described in prior publications (Dale & Sereno, 1993; Dale et al., 1999; Fischl et al., 1999a; Fischl et al., 1999b; Fischl and Dale, 2000; Fischl et al., 2001; Fischl et al., 2002; Fischl et al., 2004a; Fischl et al., 2004b; Ségonne et al., 2004; Han et al., 2006; Jovicich et al., 2006; Reuter et al. 2010; Reuter et al. 2012). Briefly, this processing includes motion correction and averaging (Reuter et al. 2010) of two volumetric T1-weighted images, removal of non-brain tissue using a hybrid watershed/surface deformation procedure (Ségonne et al., 2004), automated Talairach transformation, segmentation of the subcortical white matter and deep gray matter volumetric structures (Fischl et al., 2002; Fischl et al., 2004a), intensity normalization (Sled et al., 1998), tessellation of the gray matter white matter boundary, automated topology correction (Fischl et al., 2001; Ségonne et al., 2007), and surface deformation following intensity gradients to optimally place the gray/white and gray/cerebrospinal fluid borders at the location where the greatest shift in intensity defines the transition to the other tissue class (Dale and Sereno, 1993; Dale et al., 1999; Fischl and Dale, 2000). Once the cortical models were complete, a number of deformable procedures were performed for further data processing and analysis including surface inflation (Fischl et al., 1999a), registration to a spherical atlas which is based on individual cortical folding patterns to match cortical geometry across subjects (Fischl et al., 1999b), parcellation of the cerebral cortex into units with respect to gyral and sulcal structure (Fischl et al., 2004b; Desikan et al., 2006), and creation of a variety of surface based data including maps of curvature and sulcal depth. This method uses both intensity and continuity information from the entire three dimensional MR volume in segmentation and deformation procedures to produce representations of cortical thickness, calculated as the closest distance from the gray/white boundary to the gray/cerebral spinal fluid boundary at each vertex on the tessellated surface (Fischl and Dale, 2000). The maps are created using spatial intensity gradients across tissue classes and are therefore not simply reliant on absolute signal intensity. The maps produced are not restricted to the voxel resolution of the original data thus are capable of detecting submillimeter differences between

groups. Procedures for the measurement of cortical thickness have been validated against histological analysis (Rosas et al., 2002) and manual measurements (Kuperberg et al., 2003; Salat et al., 2004). Freesurfer morphometric procedures have been demonstrated to show good test-retest reliability across scanner manufacturers and across field strengths (Han et al., 2006; Reuter et al., 2012).

Multiple comparison correction was performed using the command line tool mri_glmfit-sim in FreeSurfer. This uses a pre-cached data simulation to measure the distribution of the maximum cluster size under the null hypothesis. Briefly, a z-map is synthesized using matched smoothing and thresholding procedures of the original analysis (10mm and $p < 0.05$, respectively). Then, areas of maximum cluster size were recorded under these parameters. This procedure was repeated for 10,000 iterations per hemisphere. Once the distributions of the maximum cluster size across simulations was obtained, multiple comparison correction was performed, which identified clusters in the original statistical maps where the clusterwise *p*-value is defined as the probability of seeing a maximum cluster of that size or larger during the simulation ($p < 0.05$).

Automated labels provided by FreeSurfer were manually checked for accuracy. This data was analyzed with version 5.1 of Freesurfer on Macintosh workstations using the Linux CentOS 5.4 operating system.

## Supplementary Results

### Relationship between Obesity PRS and Body Mass Index (BMI)

Given that the obesity PRS under investigation was derived from a GWAS of BMI, we tested the strength of its association with BMI, as a continuous variable, in these data. This regression analysis revealed that controlling for the top two PCs and sex, the obesity PRS was significantly associated with BMI ($\beta = .17$, $p = .021$).

### Potential Confounds of Obesity PRS X PTSD on Metabolic Syndrome (MetS)

We examined the following potential confounds of the Obesity PRS X PTSD effect on MetS factor scores: educational attainment, current cigarette use, and current anti-depressant use. These variables were (separately) added to the first step of the regression. Of these, only education was significantly associated with MetS (β = -.13, $p$ = .024), but the main effects of latent PTSD severity (β = .14, $p$ = .0316), obesity PRS (β = .16, $p$ = .006), and their interaction (β = .78, $p$ = .016) remained statistically significant with these additional covariates included in the model.

Given recent recommendations to test for interactions between covariates, environmental variables, and genetic moderators (Keller, 2014), we also tested all possible interactions between the environment (PTSD) and each covariate (top two PCs, sex, age) and between the PRSs and these covariates. We observed a statistically significant interaction between the PRS and sex ($p$ = .005), and therefore, we reran our main analysis with this interaction term included. Doing so did not alter our primary finding of a significant interaction between PRS and PTSD ($p$ = .04).

We also examined if the association between PTSD and MetS might be due to shared genetic effects operating on both PTSD and MetS (i.e., GE correlation) and potentially masquerading as G X E so we regressed PTSD on obesity PRS, controlling for age, sex, the top two PCs, and trauma exposure. We found no evidence that the obesity-associated genetic variation evidenced shared effects on PTSD ($p$ = .94).

**Specificity of the PTSD X Obesity PRS Effect**

We evaluated if lifetime diagnoses of major depressive disorder, generalized anxiety disorder, panic disorder, or alcohol-use disorders (abuse or dependence), as assessed with the Structured Clinical Interview for *DSM-IV* Disorders (SCID; First et al., 1997; Spitzer et al., 1998) evidenced main effects in predicting MetS and/or if they interacted with obesity PRS to predict MetS. The prevalence of these conditions in this sample was as follows: major depression = 48.5%, generalized anxiety disorder = 5.1%, panic disorder = 8.7%, and alcohol-use disorders =

62.2%. We found no evidence of an association between any of these psychiatric conditions and MetS, alone, or in interaction with obesity PRS, suggesting the specificity of the association to PTSD. We also examined dimensional indicators of depression and anxiety symptom severity (via total scores on the self-report Depression Anxiety Stress Scales; DASS; Lovibond & Lovibond, 1995) and lifetime alcohol use (via the total score on the self-report Lifetime Drinking History; LDH; Skinner, 1979) in separate regression analyses. We found that neither of these scales, either alone or in interaction with obesity PRS, was significantly associated with MetS, controlling for latent PTSD severity.

**Potential Confounds of Obesity PRS X MetS on Cortical Thickness**

We evaluated potential confounds in our interaction analysis (Keller, 2014) that could arise as a function of interactions between the covariates included in the main analysis and MetS and between the covariates and the obesity PRS on cortical thickness. Specifically, we conducted a follow-up analysis with each potential two-way interaction term included in the model (e.g., obesity PRS X PC1, MetS by PC1, etc) predicting the extracted cortical thickness values in left rostral middle frontal gyrus. This analysis yielded 1 significant interaction term for obesity PRS X age on cortical thickness values ($p = .048$). However, in a subsequent analysis that included both that interaction term and obesity PRS X MetS, the only significant interaction effect was the hypothesized one (i.e., obesity PRS X MetS: $p < .001$).

We also evaluated if current PTSD diagnosis (i.e., case/control status) might be associated with cortical thickness in the regions identified in the whole-brain analyses to determine if potential PTSD effects might have been missed by our exclusive focus on latent lifetime PTSD severity scores. Specifically, given that main effects for the obesity PRS and MetS were found in left temporal pole and right middle temporal gyrus (model 2 in Table 3) and interaction effects were observed for obesity PRS X MetS on left rostral middle frontal gyrus (model 3 in Table 3), we re-ran these analyses predicting extracted thickness values for these clusters but including current PTSD diagnosis in place of latent PTSD severity factor scores.

Similar to our main results using latent PTSD severity, we found that PTSD diagnosis was not associated with left temporal pole ($p$ = .40), right middle temporal gyrus ($p$ = .45), or left rostral middle frontal gyrus ($p$ = .71). In contrast, the main effects of obesity PRS and MetS were still evident on left temporal pole and right middle temporal gyrus (all $p$s < .001) and the interaction between obesity PRS and MetS continued to be significantly associated with left rostral middle frontal gyrus ($p$ < .001). Thus, results suggesting effects for obesity PRS, MetS, and their interaction on cortical thickness held regardless if PTSD diagnosis or severity was included as a covariate.

Separately, we also evaluated if educational attainment, total number of lifetime traumatic brain injuries, current cigarette use, and lifetime diagnoses of major depression or alcohol abuse or dependence accounted for the effects of Obesity PRS by MetS on cortical thickness in left rostral middle frontal gyrus. Including these covariates in the first step of the regression revealed that none of these variables were significantly associated with cortical thickness while Obesity PRS X MetS continued to evidence a strong and significant association ($p$ < .001). As well, we examined potential effects of dimensional (e.g., severity) indicators of depression/anxiety and, separately, alcohol use (via the self-report DASS and LDH, respectively; see above) in separate analyses. We found that neither of these variables (either alone or in interaction with the obesity PRS or in interaction with MetS factor scores) was significantly associated with cortical thickness in the left temporal pole, right middle temporal gyrus, or left rostral middle frontal gyrus (smallest $p$ = .25).

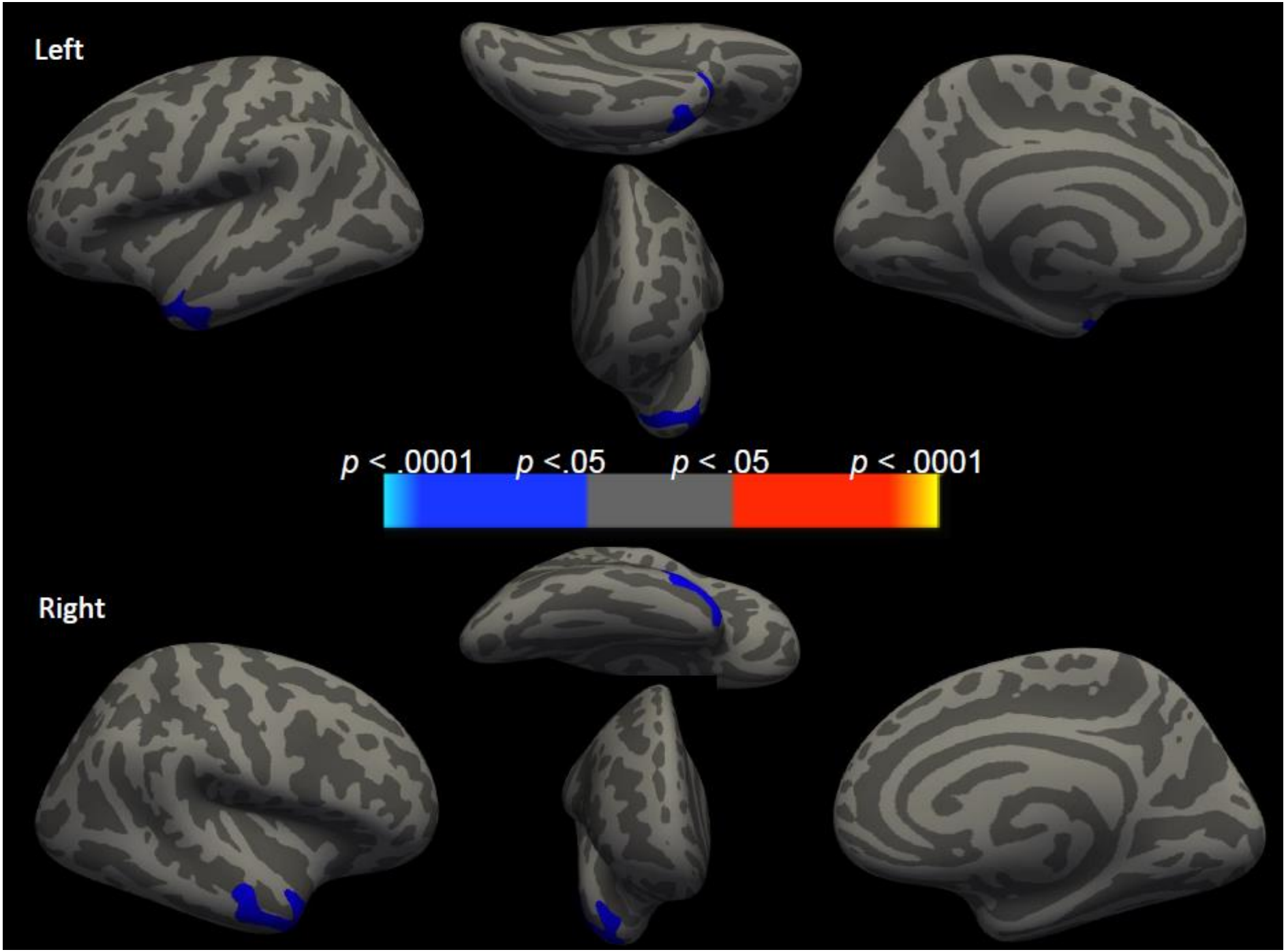


Figure S1 shows the main effects of the obesity polygenic risk score on cortical thickness controlling for PTSD and metabolic syndrome factor scores, age, sex, and the top two PCs. From left to right, the images shown represent lateral, bottom, front, and medial views.

## References

**Dale AM, Fischl B, Sereno MI** (1999). Cortical surface-based analysis I. Segmentation and surface reconstruction. *NeuroImage* **9**, 179-194.

**Dale AM, Sereno M** (1993). Improved ~~localizadon~~localization of cortical activity by combining EEG and MEG with MRI cortical surface reconstruction: a linear approach. *Journal of Cognitive Neuroscience* **5**, 162-176.

**Desikan RS, Ségonne F, Fischl B, Quinn BT, Dickerson BC, Blacker D, Buckner RL, Dale AM, Maguire RP, Hyman BT, Albert MS, Killiany RJ** (2006). An automated labeling system for subdividing the human cerebral cortex on MRI scans into gyral based regions of interest. *NeuroImage* **31**, 968-980.

**First MB, Spitzer RL, Gibbon M, Williams JB** (1997). User's guide for the Structured Clinical Interview for DSM-IV Axis I Disorders SCID-I: Clinician Version. American Psychiatric Publishing, Inc: Washington, D.C.

**Fischl B, Dale AM** (2000). Measuring thickness of the human cerebral cortex from magnetic resonance images. *Proceedings of the National Academy of Sciences of the United States of America* **97**, 11050-11055.

**Fischl B, Liu A, Dale AM** (2001). Automated manifold surgery: constructing geometrically accurate and topologically correct models of the human cerebral cortex. *IEEE Transactions on Medical Imaging* **20**, 70-80.

**Fischl B, Salat DH, Busa E, Albert M, Dieterich M, Haselgrove C, van der Kouwe A, Killiany R, Kennedy D, Klaveness S, Montillo A, Makris N, Rosen B, Dale AM** (2002). Whole brain segmentation: automated labeling of neuroanatomical structures in the human brain. *Neuron* **33**, 341-355.

**Fischl B, Salat DH, van der Kouwe AJ, Makris N, Ségonne F, Quinn BT, Dale AM** (2004a). Sequence-independent segmentation of magnetic resonance images. *NeuroImage* **23**, S69-S84.

**Fischl B, Sereno MI, Dale AM** (1999a). Cortical surface-based analysis. II: Inflation, flattening, and a surface-based coordinate system. *NeuroImage* **9**, 195-207.

**Fischl B, Sereno MI, Tootell RB, Dale AM** (1999b). High-resolution intersubject averaging and a coordinate system for the cortical surface. *Human Brain Mapping* **8**, 272-284.

**Fischl B, van der Kouwe A, Destrieux C, Halgren E, Ségonne F, Salat DH, Busa E, Seidman LJ, Goldstein J, Kennedy D, Caviness V, Makris N, Rosen B, Dale AM** (2004b). Automatically parcellating the human cerebral cortex. *Cerebral Cortex (New York, NY:1991)* **14**, 11-22.

**Han X, Jovicich J, Salat D, van der Kouwe A, Quinn B, Czanner S, Busa E, Pacheco J, Albert M, Killiany R, Maguire P, Rosas D, Makris N, Dale A, Dickerson B, Fischl B** (2006). Reliability of MRI-derived measurements of human cerebral cortical thickness: the effects of field strength, scanner upgrade and manufacturer. *NeuroImage* **32**, 180-194.

**Howie BN, Donnelly P, Marchini J** (2009). A flexible and accurate genotype imputation method for the next generation of genome-wide association studies. *PLoS Genetics* **5**, e1000529.

**Howie B, Fuchsberger C, Stephens M, Marchini J, Abecasis GR** (2012). Fast and accurate genotype imputation in genome-wide association studies through pre-phasing. *Nature Genetics* **44**, 955-959.

**Howie B, Marchini J, Stephens** (2011). Genotype imputation with thousands of genomes. *G3 (Bethesda)* **1**, 457-470.

**Jovicich J, Czanner S, Greve D, Haley E, van der Kouwe A, Gollub R, Kennedy D, Schmitt F, Brown G, Macfall J, Fischl B, Dale A** (2006). Reliability in multi-site structural MRI studies: effects of gradient non-linearity correction on phantom and human data. *NeuroImage* **30**, 436-443.

**Keller MC** (2014). Gene x environment interaction studies have not properly controlled for potential confounders: the problem and the (simple) solution. *Biological Psychiatry* **75**, 18-24.

**Kuperberg GR, Broome MR, McGuire PK, David AS, Eddy M, Ozawa F, Goff D, West WC, Williams SC, van der Kouwe AJ, Salat DH, Dale AM, Fischl B** (2003). Regionally localized thinning of the cerebral cortex in schizophrenia. *Archives of General Psychiatry* **60**, 878-888.

**Lovibond SH, Lovibond PF** (1995). Manual for Depression Anxiety Stress Scales (2nd Ed.). Psychology Foundation: Sydney.

**Marchini J, Howie B** (2010). Genotype imputation for genome-wide association studies. *Nature Reviews Genetics* **11**, 499-511.

**Reuter M, Rosas HD, Fischl B** (2010). Highly accurate inverse consistent registration: a robust approach. *NeuroImage* **53**, 1181-1196.

**Reuter M, Schmansky NJ, Rosas HD, Fischl B** (2012). Within-subject template estimation for unbiased longitudinal image analysis. *NeuroImage* **61**, 1402-1418.

**Rosas HD, Liu AK, Hersch S, Glessner M, Ferrante RJ, Salat DH, van der Kouwe A, Jenkins BG, Dale AM, Fischl B** (2002). Regional and progressive thinning of the cortical ribbon in Huntington's disease. *Neurology* **58**, 695-701.

**Salat DH, Buckner RL, Snyder AZ, Greve DN, Desikan RS, Busa E, Morris JC, Dale AM, Fischl B** (2004). Thinning of the cerebral cortex in aging. *Cerebral Cortex (New York, NY: 1991)* **14**, 721-730.

**Ségonne F, Dale AM, Busa E, Glessner M, Salat D, Hahn HK, Fischl B** (2004). A hybrid approach to the skull stripping problem in MRI. *NeuroImage* **22**, 1060-1075.

**Ségonne F, Pacheco J, Fischl B** (2007). Geometrically accurate topology-correction of cortical surfaces using nonseparating loops. *IEEE Transactions on Medical Imaging* **26**, 518-529.

**Skinner HA** (1979). Lifetime drinking history: Administration and scoring guidelines. Addiction Research Foundation: Toronto, Canada.

**Sled JG, Zijdenbos AP, Evans AC** (1998). A nonparametric method for automatic correction of intensity nonuniformity in MRI data. *IEEE Transactions on Medical Imaging* **17**, 87-97.

**Speliotes EK, Willer CJ, Berndt SI, Monda KL, Thorleifsson G, Jackson AU, Lango Allen H, Lindgren CM, Luan J, Mägi R, Randall JC, Vedantam S, Winkler TW, Qi L, Workalemahu T, Heid IM, Steinthorsdottir V,** et al. (2010). Association analyses of 249,796 individual reveal 18 new loci associated with body mass index. *Nature Genetics* **42**, 937-948.

**Spitzer RL, Gibbon M, Williams JB** (1998). Structured Clinical Interview for DSM-IV Axis I Disorders: Patient Edition (February 1996 Final), SCID-I/P. Biometrics Research, New York State Psychiatric Institute: New York.